

Article

Variability in the Water Footprint of Arable Crop Production across European Regions

Anne Gobin ^{1,*}, Kurt Christian Kersebaum ², Josef Eitzinger ³, Miroslav Trnka ^{4,5}, Petr Hlavinka ^{4,5}, Jozef Takáč ⁶, Joop Kroes ⁷, Domenico Ventrella ⁸, Anna Dalla Marta ⁹, Johannes Deelstra ¹⁰, Branislava Lalić ¹¹, Pavol Nejedlik ¹², Simone Orlandini ⁹, Pirjo Peltonen-Sainio ¹³, Ari Rajala ¹³, Triin Saue ¹⁴, Levent Şaylan ¹⁵, Ruzica Stričević ¹⁶, Višnja Vučetić ¹⁷ and Christos Zoumides ¹⁸

¹ Flemish Institute for Technological Research (VITO), 2400 Mol, Belgium

² Leibniz Centre for Agricultural Landscape Research (ZALF), 15374 Müncheberg, Germany; ckersebaum@zalf.de

³ Institute of Meteorology, University of Natural Resources and Life Sciences, 1180 Vienna, Austria; josef.eitzinger@boku.ac.at

⁴ Global Change Research Institute, The Czech Academy of Sciences, 61300 Brno, Czech Republic; mirek_trnka@yahoo.com (M.T.); phlavinka@centrum.cz (P.H.)

⁵ Department of Agrosystems and Bioclimatology, Mendel University in Brno, 61300 Brno, Czech Republic

⁶ National Agricultural and Food Centre, Soil Science and Conservation Research Institute, Bratislava 82713, Slovakia; j.takac@vupop.sk

⁷ Wageningen Environmental Research (Alterra), 6700 AA Wageningen, The Netherlands; joop.kroes@wur.nl

⁸ Consiglio per la Ricerca in Agricoltura e L'analisi Dell'economia Agraria, Unità di Ricerca per i Sistemi Culturali degli Ambienti Caldo-Aridi, 70125 Bari, Italy; domenico.ventrella@crea.gov.it

⁹ Department of Agrifood Production and Environmental Sciences (DISPAA), University of Florence, 50155 Florence, Italy; anna.dallamarta@unifi.it (A.D.M.); simone.orlandini@unifi.it (S.O.)

¹⁰ Norwegian Institute of Bioeconomy Research (NIBIO), 1431 Ås, Norway; johannes.deelstra@nibio.no

¹¹ Faculty of Agriculture, University of Novi Sad, Novi Sad 21000, Serbia; branislava.lalic@df.uns.ac.rs

¹² Earth Science Institute of Slovak Academy of Science, Bratislava 84005, Slovakia; nejedlik@yahoo.com

¹³ Natural Resources Institute Finland (Luke), 31600 Jokioinen, Finland; pirjo.peltonen-sainio@luke.fi (P.P.-S.); ari.a.rajala@luke.fi (A.R.)

¹⁴ Estonian Crop Research Institute, Tallinn Technical University, Jõgeva 48309, Estonia; triin.saue@etki.ee

¹⁵ Department of Meteorology, Faculty of Aeronautics and Astronautics, Istanbul Technical University, 34469 Istanbul, Turkey; saylan@itu.edu.tr

¹⁶ Faculty of Agriculture, University of Belgrade, Zemun-Belgrade 11080, Serbia; sruzica@agrif.bg.ac.rs

¹⁷ Meteorological and Hydrological Service, Zagreb 10000, Croatia; vucetic@cirus.dhz.hr

¹⁸ Energy, Environment & Water Research Center, The Cyprus Institute, Nicosia 2121, Cyprus; c.zoumides@cyi.ac.cy

* Correspondence: anne.gobin@vito.be; Tel.: +32-14-336775

Academic Editor: Ashok K. Chapagain

Received: 24 October 2016; Accepted: 31 January 2017; Published: 8 February 2017

Abstract: Crop growth and yield are affected by water use during the season: the green water footprint (WF) accounts for rain water, the blue WF for irrigation and the grey WF for diluting agri-chemicals. We calibrated crop yield for FAO's water balance model "Aquacrop" at field level. We collected weather, soil and crop inputs for 45 locations for the period 1992–2012. Calibrated model runs were conducted for wheat, barley, grain maize, oilseed rape, potato and sugar beet. The WF of cereals could be up to 20 times larger than the WF of tuber and root crops; the largest share was attributed to the green WF. The green and blue WF compared favourably with global benchmark values ($R^2 = 0.64\text{--}0.80$; $d = 0.91\text{--}0.95$). The variability in the WF of arable crops across different regions in Europe is mainly due to variability in crop yield ($\overline{cv} = 45\%$) and to a lesser extent to variability in crop water use ($\overline{cv} = 21\%$). The WF variability between countries ($\overline{cv} = 14\%$) is lower than the variability between seasons ($\overline{cv} = 22\%$) and between crops ($\overline{cv} = 46\%$). Though modelled yields

increased up to 50% under sprinkler irrigation, the water footprint still increased between 1% and 25%. Confronted with drainage and runoff, the grey WF tended to overestimate the contribution of nitrogen to the surface and groundwater. The results showed that the water footprint provides a measurable indicator that may support European water governance.

Keywords: water footprint; arable crops; cereals; Europe; crop water use; yield

1. Introduction

The water footprint (WF) concept has created awareness of sustainable water use following a global assessment of national production, consumption and international trade [1]. Traditional water consumption statistics have been given for different sectors, such as domestic, agricultural and industrial water use, but these show little about how much water is actually used. The water footprint provides a way to compare water use of regions, sectors, commodities and nations. Leading work in understanding water availability and risk has come from the food industries through the analysis of water quantities that companies use throughout their supply chain. With water being inherently local, the water footprint calculations highlight the risks of local exploitations that could potentially disrupt both business operations and the surrounding community.

Water is a precious commodity, certainly in drought-prone regions and at times of drought in any part of the world. The economic cost of drought has been enormous. In 2003, combined drought and heat waves led to 30% reduction in primary productivity [2], and an estimated 13 billion € loss in European agricultural production [3]. With water shortages already threatening growth, the future of Europe's agriculture will be tied closely to water availability. In addition climate models project that southern Europe will face increased drought and central Europe prolonged dry spells [4,5] frequently combined with heat waves [6]. The rising population, coupled with increasing demands by the agriculture and energy industries presents an interdependent relationship often referred to as the water–food–energy nexus; the demand for water will likely outweigh supply by 2050 unless changes in food and energy preferences are implemented [7]. While access to water has been recognized as a basic human right, the increasingly high demand for water resources should be valued according to its supply.

The WF is closely linked to the concept of virtual water, which is the volume needed to produce a commodity or service. Importing virtual water can be perceived as a partial solution to problems of water scarcity, particularly in dry regions [8]. National, regional and global water and food security can be improved when water-intensive commodities are traded from places where they are economically viable to places they are not. Food import offers an alternative to reduce pressure on domestic water resources and enables more productive water use as expressed by the WF of food [9]. Other research has taken a life cycle assessment (LCA) approach to evaluate the water footprint of products, processes and organisations as initiated by [10]. Subsequently, an ISO 14046 standard was set to specify the principles, requirements and guidelines [11]. The ISO standard may introduce complexity by creating water footprints for each environmental impact, e.g., for water availability, scarcity, eutrophication and eco-toxicity, across the life cycle of a product which is beyond the crop water footprint that this research focuses on.

The WF of crops forms the basis for WF estimations of crop products and derived commodities [12]. In terms of water volumes used, the crop WF estimations consider three major sources of water, i.e., water from rain (green WF), irrigation (blue WF) and water for diluting chemicals (grey WF) [13]. In a comparison of different irrigation and water conservation methods for four locations [14], it was concluded that a combination of drip irrigation and synthetic mulching allowed for the largest reduction in the WF of maize, potato and tomato. The inter-annual variability of the crop WF highlighted inter alia the importance of increased yields for 22 crops for the period 1978–2008 in

China [15]. Understanding the variability is a prerequisite to making projections of good water governance under different scenarios of global change. Our study contributes to understanding the variability of the WF across regions, soils and annual weather conditions in Europe. We hypothesize that the variability in the water footprint of arable crops across different regions in Europe is mainly due to variability in crop yield and to a lesser extent to variability in crop water use. Therefore, the objectives of this study were to quantify the variability in water used to grow arable crops across different regions in Europe; to estimate their yield variability; to establish the variability in the WF of these different crops; and, to compare the results with benchmark values from global model estimates as in [16]. Understanding the sources of variability in the WF is important to elucidate water consumption patterns in relation to crop production, which in turn enables more efficient water management and agricultural water governance within the framework of a water–food–energy nexus.

2. Materials and Methods

2.1. Data

We collected temperature, rainfall, wind speed, solar radiation and relative humidity data from 41 meteorological stations across different regions in Europe for the period 1992–2012 (Table 1; Figure 1). Reference evapotranspiration was calculated using the modified Penman-Monteith approach [17]. The climatological diagrams of temperature, precipitation and evapotranspiration for these locations demonstrate a wide variation in weather conditions (Figure 2) and soils (Appendix A). The dominant soil type(s) for 45 locations were described in terms of texture; chemical composition; volumetric water content at saturation, field capacity and wilting point of different soil horizons up to 1.5 m or to an impervious layer. With the exception of polder regions, groundwater was absent and water leaching from the root zone was discharged as drainage. In each location major arable crops were selected for calculating the water footprint (Table 1).

Table 1. Meteorological stations and crops per region (Location see Figure 1).

Country	Region	Meteo Stations ¹	Major Crops ²
AT	Marchfeld	Gross Enzersdorf, Fuchsenbigl	WHB, BAR, MAZ, SBT
BE	Flanders	Koksijde, Gent, Ukkel, Peer	WHB, BAR, MAZ, SBT, POT
CY	Country	Nicosia, Pafos, Larnaca	WHD, POT, BAR, MAZ
CZ	Eastern Czech	Domaninek, Lednice, Verovany	WHB, BAR, MAZ, RAP
DE-1	Märk. Oderland	Muncheberg , Manschnow	WHB, BAR, SBT, RAP, POT, MAZ
DE-2	North-East Lower Saxony	Braunschweig	WHB, BAR, SBT
EE	Country	Kuusiku , Tartu, Tallinn, Võru, Pärnu, Väike-Maarja, Kuressaare	WHB, BAR, POT, RAP
FI-1	Häme	Jokioinen	BAR, WHB, BAR, POT, RAP
FI-2	South Finland	Mikkeli, Ylistaro, Laukaa, Piikio	BAR, WHB, BAR, POT, RAP
HR	Koprivnica-Križevci	Križevci	MAZ
IT-1	Foggia	Foggia	WHD, SBT
IT-2	Val d'Orcia	Radicofani	WHB, WHD, BAR
NO	South Eastern Norway	Søråsjordet	BAR
NL	Flevoland	Lelystad	WHB, POT, SBT, MAZ
PL	Mazovia	Dąbrowice	WHB, BAR, POT, SBT, RAP
SK	Danube Lowland	Bratislava-letisko , Hurbanovo, Nitra, Jaslovske Bohunice	WHB, BAR, MAZ
SR	Vojvodina	Rimski Sancevi	WHD, MAZ, SBT, POT
TR	Thrace	Edirne, Kırklareli , Tekirdağ	WHD, WHB, BAR, MAZ

Notes: ¹ In bold are meteorological stations located in the vicinity of experimental fields; ² BAR is barley (*Hordeum vulgare* L.); MAZ is maize (*Zea mays* L.); POT is potato (*Solanum tuberosum* L.); SBT is sugar beet (*Beta vulgaris* L.); RAP is oilseed rape (*Brassica napus* L.); WHB is common wheat (*Triticum aestivum* L.); and, WHD is durum wheat (*Triticum turgidum* L.).

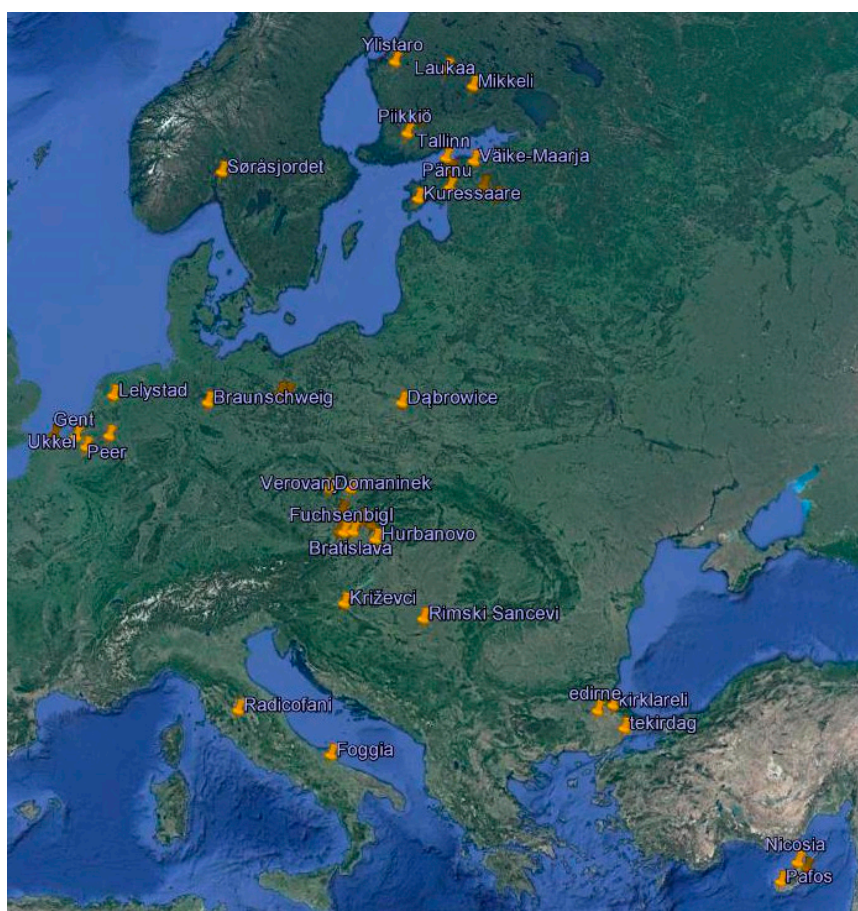


Figure 1. Location of different meteorological stations across Europe.

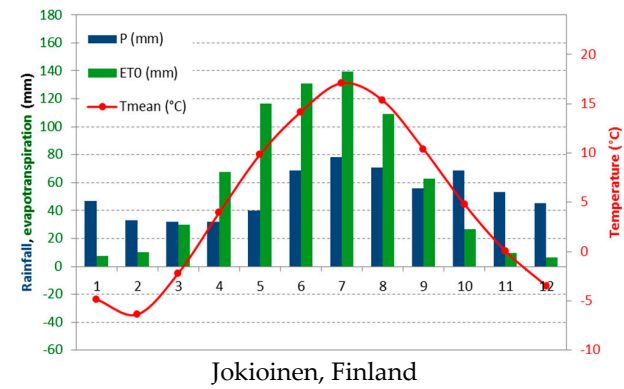
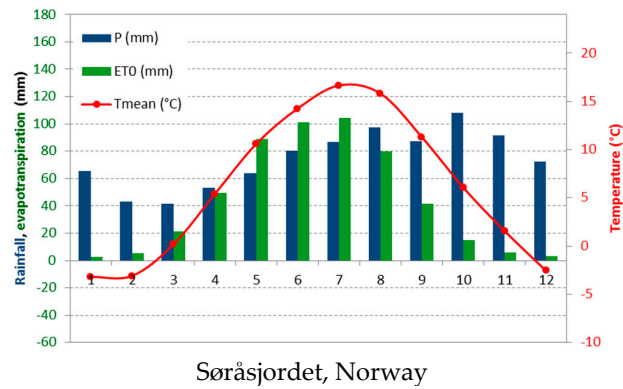
2.2. Crop Water Use

FAO's "Aquacrop" model version 5.0 [18] was used to calculate the crop water footprint. The growth module is evapotranspiration driven, where crop transpiration (T) is converted to biomass through a water productivity parameter [19,20]. The evaporative power of the atmosphere (ET_0) is converted to actual evapotranspiration (ET) and separated into non-productive water fluxes, i.e., soil evaporation (E), and productive water fluxes, i.e., crop transpiration (T). Soil moisture conditions determine E from the soil surface not covered by canopy [19,20]. Crop canopy expands from seedling to maturity as determined by accumulated growing degree days.

Crop calendar and growth characteristics were collected for the major arable crops in each location (Table 1). The crop growth parameters were set using experimental field data collected for each region (Appendix A, [21]). For regions without experimental field data available, crop growth parameters were derived from farmers' fields' data.

All weather, soil and crop input data (Figure 2; Appendix A) were inserted into the model. The model's phenological module was run in growing degree days to capture crop growth dynamics during the growing season. Rainfed model runs for the different locations were followed by sprinkler irrigation runs, at 80% field capacity, and according to local farm practices. Therefore, regions where no irrigation was reported were excluded from the irrigation model runs.

Northern Europe (EE, FI, NO)



Western Europe (BE, DE, NL)

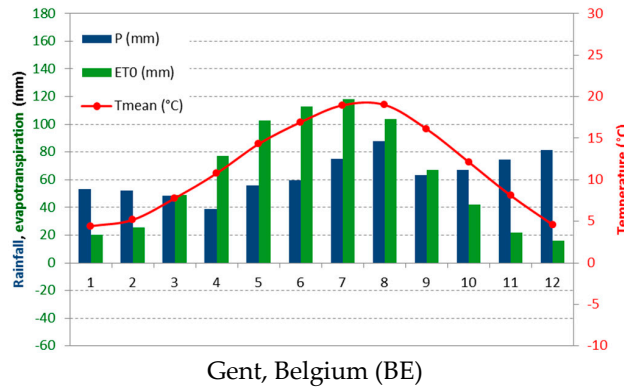
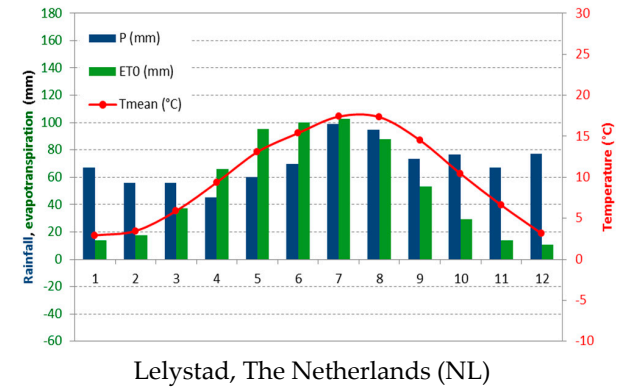
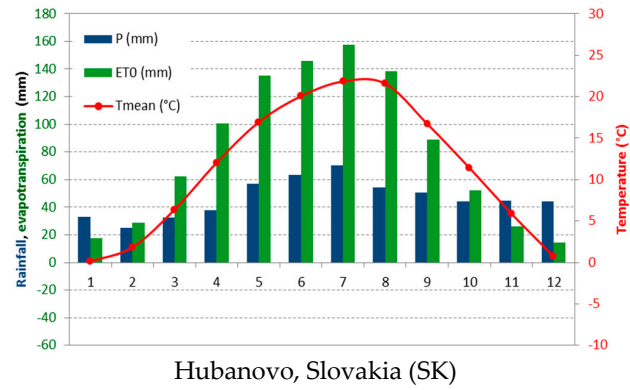
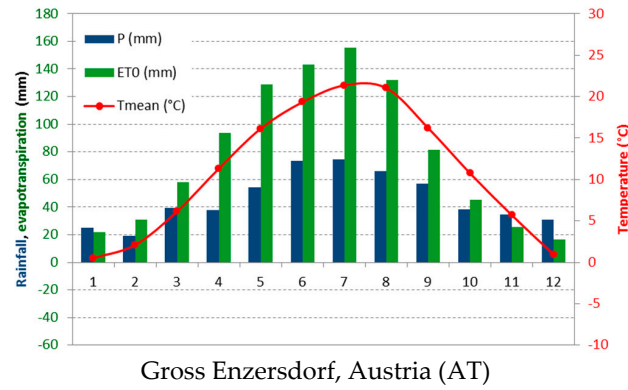


Figure 2. Cont.

Central Europe (AT, CZ, DE, SK)



South Europe (CY, HR, IT, SR, TR)

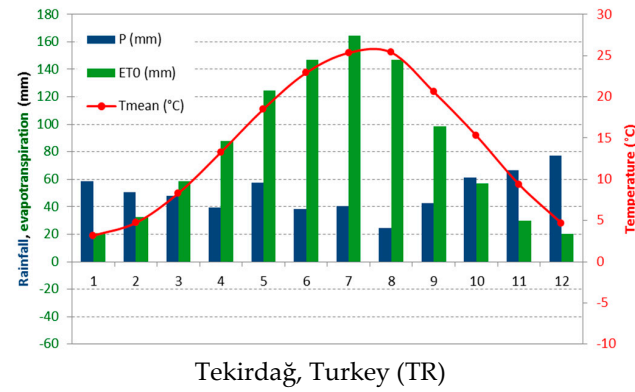
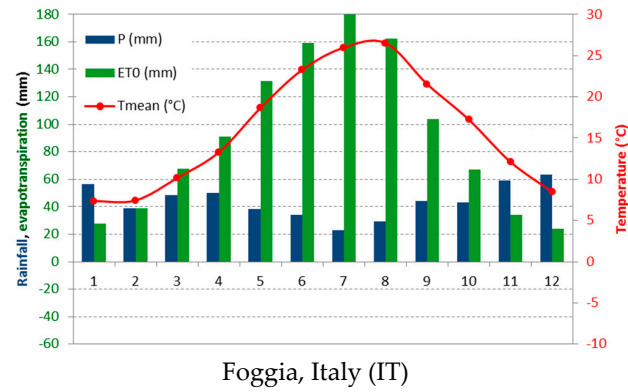


Figure 2. Climatological diagrams for different meteorological stations along a broad transect in Europe for the period 1992–2012. *P* is precipitation (mm); *ET0* is reference evapotranspiration (mm); *Tmean* is average temperature (°C). A two letter code refers to the countries.

2.3. Water Footprint Calculations

Irrigated agriculture receives water from irrigation (blue water) and from precipitation (green water), while rainfed agriculture only receives green water. Green water is originated by precipitation and is the soil water held in the unsaturated zone available to plants, while blue water refers to the manageable water in rivers, lakes, wetlands and aquifers [22]. The green WF and blue WF reflect the rainfed and irrigated crop water use per harvested crop with calculation methods established by [13]. The grey WF accounts for water used to dilute nutrient pollution to meet ambient water quality standards; for reasons of comparison we focused on nitrogen pollution [16].

$$WF_{green} = \frac{10 \cdot \sum_{d=1}^{l_{gp}} ET_{d, green}}{Y} \quad (1)$$

$$WF_{blue} = \frac{10 \cdot \sum_{d=1}^{l_{gp}} ET_{d, blue}}{Y} \quad (2)$$

$$WF_{grey} = \frac{[[\alpha \cdot AR] / [c_{max} - c_{nat}]]}{Y} \quad (3)$$

where ET_d is the daily evapotranspiration in $\text{mm} \cdot \text{day}^{-1}$, accumulated over the length of the growing period (l_{gp} , in days), under rainfed (*green*) and irrigated (*blue*) conditions. The factor 10 converts water depths from millimetres into water volumes per land surface ($\text{m}^3 \cdot \text{ha}^{-1}$). The nominator reflects crop water use in $\text{m}^3 \cdot \text{ha}^{-1}$, whereas the denominator (Y) is crop yield in $\text{Mg} \cdot \text{ha}^{-1}$. The green water evapotranspiration under irrigated conditions was estimated as the total evapotranspiration simulated in a scenario without irrigation. The blue water evapotranspiration equalled the total evapotranspiration simulated in the scenario with irrigation minus the simulated green water evapotranspiration. For the grey WF, we assumed that the nitrogen fraction (α) that reached free flowing water bodies through leaching or runoff equalled 10% of the application rate (AR in $\text{kg} \cdot \text{ha}^{-1} \cdot \text{year}^{-1}$). Fertilizer application rates were reduced significantly in the European Member States following the introduction of the Nitrates Directive in 1991 and the Water Framework Directive in 2000. Reporting mechanisms are in place so that nitrogen application rates and derived gross nitrogen balances are available from Eurostat for the period 1992–2012 [23]. Fertilizer consumption rates are available per hectare of arable land in the World Bank database [24]. We assumed drinking water standards for water quality with a difference between maximum acceptable and natural background concentration ($c_{max} - c_{nat}$) of $10 \text{ mg} \cdot \text{L}^{-1}$ [16].

2.4. Yield Statistics

Yield is an important component of the WF. Yields, area and production of wheat, barley, grain maize, potato, sugar beet and oilseed rape differed distinctly across the different regions in Europe, as shown for 2012 regional statistical yields (Figure 3). The harvested production of cereals in 2012–2015 in the EU-28 was estimated at one ninth of global cereals production; wheat (44%–47%), maize (21%–22%) and barley (19%–20%) account for a high share [25]. Despite a European-wide system of production quota, sugar beet remains the most important root crop for north-western Europe. Potato production is more widely spread across the different European Member States, as reflected by the presence of yield data in different regions (Figure 3). Oilseed rape, the main oilseed crop across Europe, showed an upward trend in production during the last decade due to its use for bioenergy purposes [25]. Regional statistical yields were compared with modelled yields assuming a humidity of 14% for cereals, 80% for root crops and 9% for oilseed rape [25].

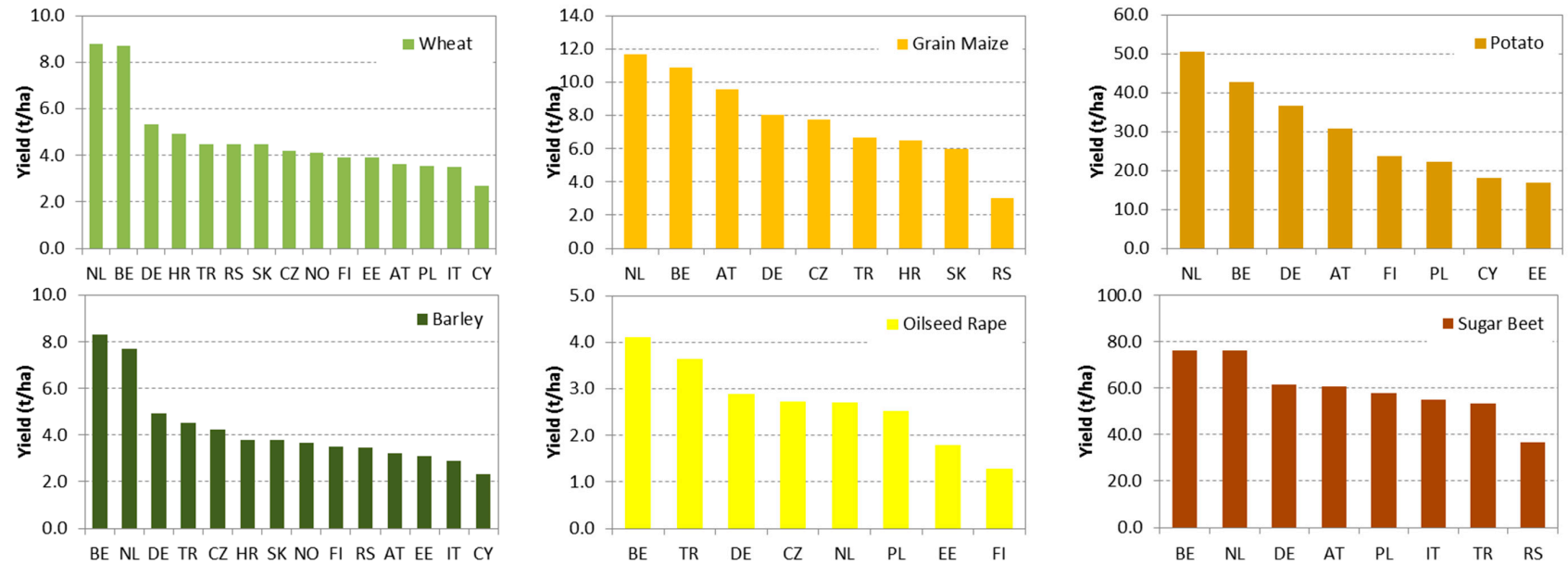


Figure 3. Yields ($\text{Mg}\cdot\text{ha}^{-1}$) for major arable crops across the European regions for the year 2012 based on regional statistics. A two letter code refers to the country that the region belongs to.

2.5. Statistical Analysis

The statistical analysis was done in R using the core functionalities [26] and the hydroGOF package [27]. Common statistical measures were used to describe the datasets. The coefficient of variation (*cv*), i.e., the ratio of the standard deviation to the mean expressed in %, was used to compare the spread of variables. The Pearson correlation coefficient (r^2) was used as a measure of strength of an association between two variables. Statistical metrics to describe the agreement between modelled and statistical yields and between our and benchmark WFs were the mean average error (MAE), the root mean square error (RMSE) and the index of agreement (*d*) [27]. The regression lines on the graphs and the associated coefficient of determination (R^2) were provided as a measure of how well the statistical yields or the benchmark WFs were approximated by our modelled results.

3. Results

The water footprint (WF) of arable crops across different regions in Europe showed a large variability. We presented this large variability in relation to the different components that comprised the water footprint: evaporation and transpiration; biomass and yield; and, the green, blue and grey WF. Since these components were intrinsically linked to the water balance, a general comparison was made of the major water balance input and output.

3.1. Water Balance

The water balance was driven by reference evapotranspiration, calculated from solar radiation, wind speed, temperature and relative humidity using the modified Penman–Monteith equation [17]. In all studied regions (Table 1), the reference evapotranspiration was higher than the precipitation accumulated over the growing season of spring sown crops (Figure 4). For autumn sown crops this difference was less pronounced. In northern and western European regions cumulative precipitation was higher than cumulative evapotranspiration during the growing season for the period 1992–2012. Simulated sub-surface drainage was in all cases higher than simulated surface runoff, but this difference was not always significant (Figure 5). A surplus on the water balance led to higher runoff and drainage during the growing season, and vice versa for a deficit. Due to higher precipitation during winter a surplus occurred during the growing season of autumn sown crops (Figure 5).

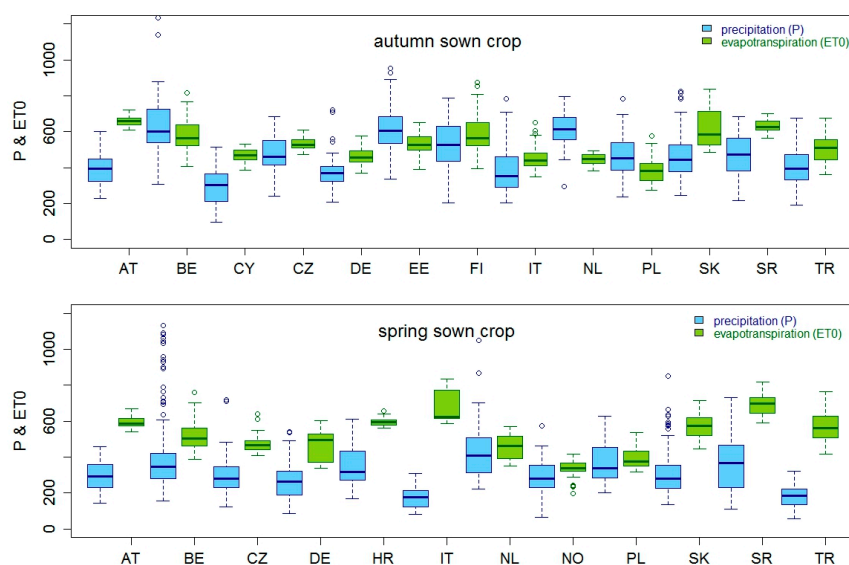


Figure 4. Precipitation (*P* in mm) and reference evapotranspiration (*ET0* in mm) during the growing season of autumn and spring sown crops across the European regions for the period 1992–2012. A two letter code refers to the country that the region belongs to.

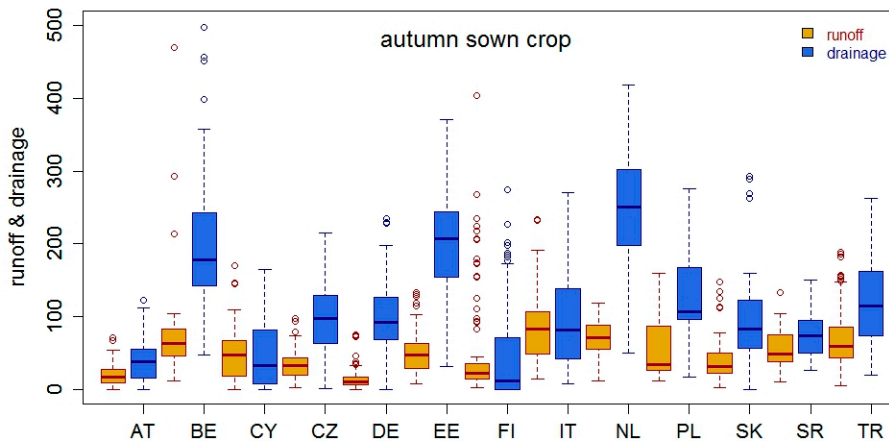


Figure 5. Runoff (mm) and drainage (mm) during the growing season of autumn sown crops across the European regions for the period 1992–2012. A two letter code refers to the country that the region belongs to.

3.2. Soil Evaporation and Crop Transpiration

The crop evapotranspiration comprised two major components, i.e., soil evaporation and crop transpiration. At sowing and planting soil evaporation was relatively high and crop transpiration low. As the growing season progresses crop transpiration represented the largest share of the evapotranspiration (Figure 6). After maturity the contribution of evaporation largely depends on the time between maturity and harvest. Overall a large variability was observed between the different European regions and was attributed mostly to transpiration. Summer crops had the largest variability (Figure 6), and this variability became less under irrigation (Figure 7).

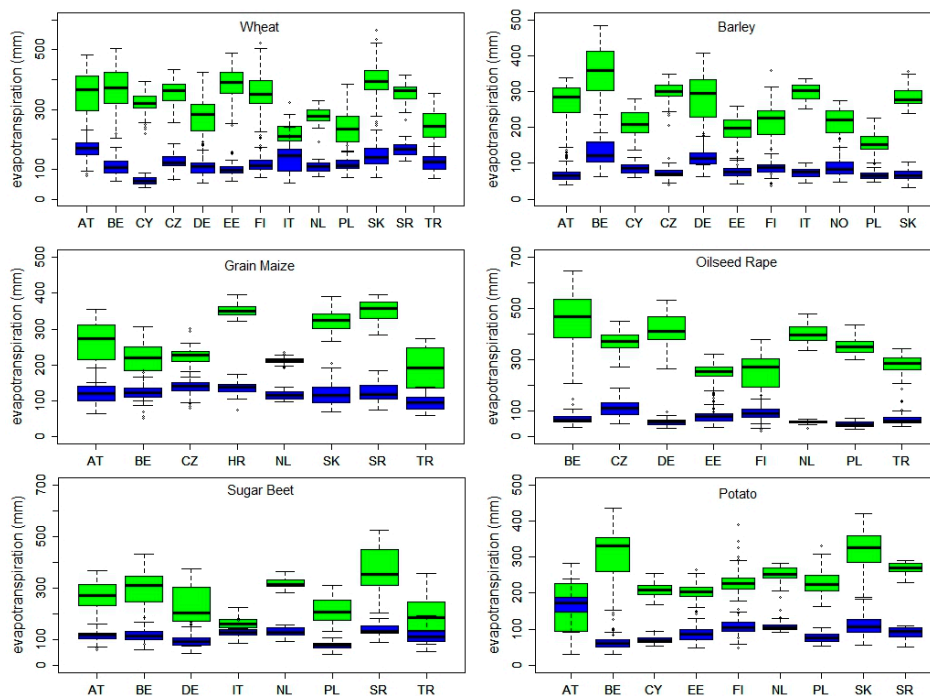


Figure 6. Transpiration (T in mm, green) and evaporation (E in mm, blue) for major arable crops across the European regions for the period 1992–2012. A two letter code refers to the country that the region belongs to.

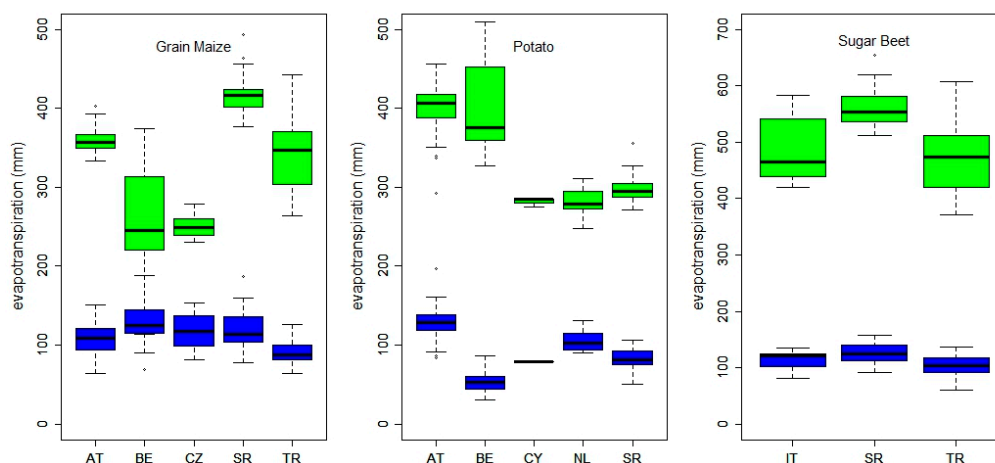


Figure 7. Transpiration (T in mm, green) and evaporation (E in mm, blue) for irrigated summer crops across the European regions for the period 1992–2012. A two letter code refers to the country that the region belongs to.

3.3. Biomass and Yield

The total biomass and yield were modelled in dry weight using “Aquacrop”. For reasons of comparison with statistical yields, modelled yield and biomass were converted to fresh weight assuming humidity at harvest of 14% for cereals, 80% for root crops and 9% for oilseed rape [25].

An overall satisfactory correspondence was observed between modelled and statistical yields (Figure 8). The modelled results relied on calibrated crop phenological and growth development on experimental fields [21] or on farmers’ fields. The best agreement between modelled and statistical yields was obtained for rapeseed ($R^2 = 0.60$; MAE = 0.7; RMSE = 0.8) and barley ($R^2 = 0.62$; MAE = 1.1; RMSE = 1.3), followed by wheat ($R^2 = 0.50$; MAE = 1.5; RMSE = 1.8) and maize ($R^2 = 0.48$; MAE = 2.1; RMSE = 2.5). Potato ($R^2 = 0.48$; MAE = 9.3; RMSE = 11.2) and sugar beet ($R^2 = 0.31$; MAE = 10.0; RMSE = 11.6) showed a weak linear relationship between modelled and statistical yields (Figure 8); where MAE is mean average error and RMSE is root mean square error [27]. All modelled crop yields were higher than the corresponding statistical yields owing in part to calibration on experimental and farmers’ fields [21], which were on average more intensively managed than the entire crop area. In addition, the statistical yields are a simple division of crop production by area harvested and therefore lead to an overall lower yield than observed on individual farms.

The modelled yields ranged from 0.56 $\text{Mg}\cdot\text{ha}^{-1}$ higher for oilseed rape to 5.5 $\text{Mg}\cdot\text{ha}^{-1}$ for potato as compared to statistical yields (Table 2). Modelled cereal yields had lower variabilities relative to the mean as compared to statistical cereal yields. Modelled root and tuber crop yields, however, had larger standard deviations than the corresponding statistical yields. For example, statistical potato yields ($28.1 \pm 12.6 \text{ Mg}\cdot\text{ha}^{-1}$) were lower and had a lower dispersion than modelled potato yields ($33.6 \pm 13.9 \text{ Mg}\cdot\text{ha}^{-1}$). The combined inter-regional and inter-annual variabilities relative to the mean were lower for modelled yields as compared to statistical yields (Table 2). The coefficient of variation was highest for statistical yields of potatoes (44.9%), closely followed by rapeseed (44.5%) and barley (42%). The lowest variability was for modelled wheat yields (17%) and statistical sugar beet yields (22%). Yields were modelled as a fraction of dry harvestable biomass, whereas comparisons between modelled and statistical yields were made on a fresh weight basis. The harvest index (HI in Table 2), i.e., the ratio between yield and biomass, enabled conversion to fresh weight biomass. In addition to humidity at harvest, conversions to fresh weight biomass assumed a humidity of 70% for green above ground biomass. After conversion, the statistical metrics standard deviation (s) and coefficient of variation (cv) for biomass were the same as for modelled and statistical yields, respectively. Higher harvest indices may occur in individual countries, and certainly occur for dry weight conversions.

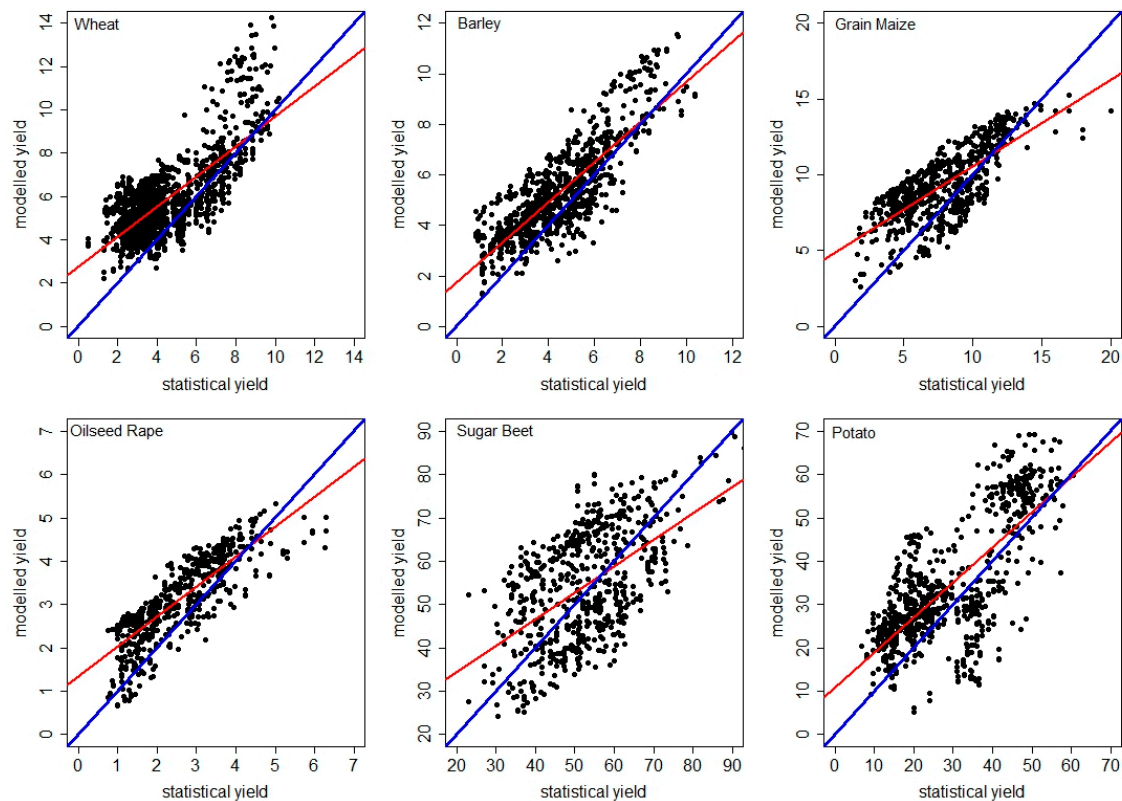


Figure 8. Comparison of modelled and statistical yields (in $\text{Mg}\cdot\text{ha}^{-1}$) and expressed in fresh weight for major arable crops across the European regions for the period 1992–2012, including the identity line (blue) and a linear regression of modelled on statistical yield (red).

Table 2. Modelled and statistical yields (in $\text{Mg}\cdot\text{ha}^{-1}$) and harvest index (HI in %) for the major arable crops in Europe for the period 1992–2012. For crop abbreviations see Figure 3.

Crop	y _{stat} ·m	y _{stat} ·s	y _{stat} ·cv	y _{mod} ·m	y _{mod} ·s	y _{mod} ·cv	HI
BAR	4.44	1.86	41.88	5.26	1.77	33.54	41
MAZ	7.76	2.92	37.67	9.28	2.27	24.50	41
POT	28.07	12.60	44.88	33.58	13.89	41.35	72
RAP	2.48	1.10	44.50	3.04	0.92	30.26	23
SBT	52.43	11.55	22.02	54.24	12.74	23.48	64
WHB	4.94	2.04	41.27	6.13	1.96	31.91	41
WHD	3.05	0.85	27.99	4.96	0.86	17.43	37

Notes: Where y is yield ($\text{Mg}\cdot\text{ha}^{-1}$); HI is harvest index (%); stat refers to regional statistics and mod to modelled; m denotes mean, s standard deviation and cv coefficient of variation (%). All figures refer to fresh weight.

3.4. Green, Blue and Grey Water Footprint

We calculated the green water footprint (WF) for rainfed crops using both modelled and statistical yields (Figure 9). Across all European regions the largest green WF was calculated for oilseed rape ($1857 \pm 661 \text{ m}^3\cdot\text{Mg}^{-1}$), durum wheat ($1414 \pm 720 \text{ m}^3\cdot\text{Mg}^{-1}$) and common wheat ($1108 \pm 580 \text{ m}^3\cdot\text{Mg}^{-1}$), followed by barley ($901 \pm 458 \text{ m}^3\cdot\text{Mg}^{-1}$) and grain maize ($590 \pm 304 \text{ m}^3\cdot\text{Mg}^{-1}$). The lowest green WFs were calculated for potatoes ($157 \pm 75 \text{ m}^3\cdot\text{Mg}^{-1}$) and sugar beet ($67 \pm 19 \text{ m}^3\cdot\text{Mg}^{-1}$). Green WF calculations with modelled yields were between 1% lower for sugar beet and up to 78% lower for durum wheat as compared to statistical yields owing to a larger variation in the statistics. The coefficient of variation was lowest for modelled sugar beet (21%) and highest for modelled wheat (44%); for statistical yields these were 29% and 52%, respectively. The largest green WF was calculated for oilseed rape in FI ($2410 \pm 727 \text{ m}^3\cdot\text{Mg}^{-1}$)

and EE ($2191 \pm 569 \text{ m}^3 \cdot \text{Mg}^{-1}$), followed by common wheat in EE ($2147 \pm 568 \text{ m}^3 \cdot \text{Mg}^{-1}$) and durum wheat in CY ($2055 \pm 1019 \text{ m}^3 \cdot \text{Mg}^{-1}$). The lowest green WF was calculated for sugar beet in AT ($61 \pm 7 \text{ m}^3 \cdot \text{Mg}^{-1}$), DE ($61 \pm 14 \text{ m}^3 \cdot \text{Mg}^{-1}$), NL ($62 \pm 8 \text{ m}^3 \cdot \text{Mg}^{-1}$) and BE ($63 \pm 11 \text{ m}^3 \cdot \text{Mg}^{-1}$).

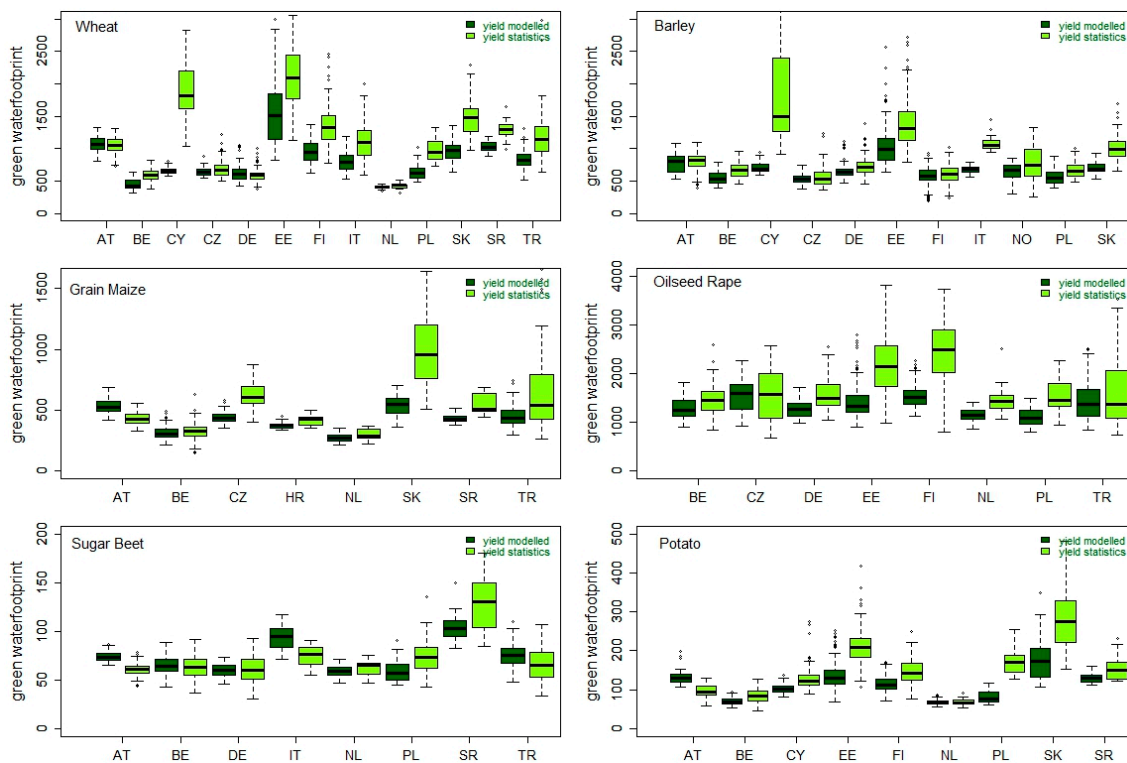


Figure 9. The green water footprint (in $\text{m}^3 \cdot \text{Mg}^{-1}$) for modelled and statistical arable yields across the European regions for the period 1992–2012. A two letter code refers to the country that the region belongs to.

Crop water use and yield, both used for calculating the green WF for rainfed crops, were significantly correlated. The Pearson correlations of statistical yields with transpiration ($r^2 = 0.33$; $p < 0.001$) were stronger than with evapotranspiration ($r^2 = 0.28$; $p < 0.001$); for modelled yields this was 0.33 and 0.31, respectively ($p < 0.001$). The green WF decreased exponentially with increasing yields, which was more pronounced for statistical yields than for modelled yields owing to the presence of extremely low yields in the statistical series. Regions with extremely low yields in their data records therefore displayed a larger variability in the green WF (Figure 9). Examples were wheat and barley in CY and EE; grain maize in SK and TR; oilseed rape in FI and EE; sugar beet in SR; and, potato in SK. The relationship between the green WF and evapotranspiration was linearly positive but extremely weak, whereas with transpiration a slightly stronger relation was observed. The variability in yields, however, dominated the green water footprint.

The combined green and blue water footprint was calculated for irrigated crops, notably grain maize, potato and sugar beet. Irrigation amounts varied between the different European regions, reflecting different climatological environments, soil types and growing seasons (Figure 10). The largest irrigation needs were estimated for sugar beet in IT ($434 \pm 70 \text{ mm}$), followed by potato in CY ($278 \pm 142 \text{ mm}$) and sugar beet in TR ($356 \pm 108 \text{ mm}$); the lowest irrigation amounts were for potato in NL ($72 \pm 47 \text{ mm}$), grain maize in BE ($92 \pm 63 \text{ mm}$) and CZ ($100 \pm 41 \text{ mm}$). A larger variation was observed for sandy textured soils such as present in BE, DE and AT. For SR, CY, TR and IT higher temperatures and evapotranspiration rates combined with low precipitation amounts resulted in larger water demands for irrigation (Figure 10). An expected strong linear relation was observed between irrigation and evapotranspiration ($r^2 = 0.77$; $p < 0.001$). Statistical yields were significantly correlated

with irrigation amounts ($r^2 = 0.27$; $p < 0.001$), evapotranspiration ($r^2 = 0.38$; $p < 0.001$) and transpiration ($r^2 = 0.45$; $p < 0.001$) during the growing season, suggesting the presence of irrigated yields in the statistical data.

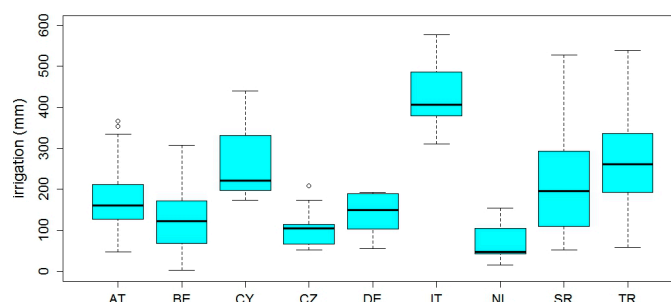


Figure 10. Irrigation (in mm) during the cropping season across the European regions for the period 1992–2012. A two letter code refers to the country that the region belongs to.

Since no statistical data were available for yields under irrigation, we could only compare modelled water footprints under irrigated and rainfed conditions. Higher evapotranspiration rates of up to 155 mm for maize in TR, 205 mm for potato in AT and 304 mm for sugar beet in IT were accompanied by higher yields of up to $3.1 \text{ Mg}\cdot\text{ha}^{-1}$ (48%) for maize in TR, $12.4 \text{ Mg}\cdot\text{ha}^{-1}$ (49%) for potato in AT and $20.7 \text{ Mg}\cdot\text{ha}^{-1}$ (50%) for sugar beet in TR. The combined increases in yields and evapotranspiration rates resulted in increases in the WFs of irrigated crops. When comparing irrigated to rainfed conditions, we estimated WF increases of between $4 \text{ m}^3\cdot\text{Mg}^{-1}$ (5%) for potato in BE and $33 \text{ m}^3\cdot\text{Mg}^{-1}$ (6%) for maize in AT; the range in percentages varied from 1% ($6 \text{ m}^3\cdot\text{Mg}^{-1}$) for maize in TR to 25% ($18 \text{ m}^3\cdot\text{Mg}^{-1}$). The WF under irrigated conditions was dominated by green water (Figure 11), which in turn was mostly influenced by yields. The highest blue and green WF was for grain maize in AT ($566 \pm 79 \text{ m}^3\cdot\text{Mg}^{-1}$) and TR ($457 \pm 59 \text{ m}^3\cdot\text{Mg}^{-1}$), followed by potato in AT ($142 \pm 18 \text{ m}^3\cdot\text{Mg}^{-1}$) and SR ($134 \pm 17 \text{ m}^3\cdot\text{Mg}^{-1}$). The lowest blue and green WFs were for potato in BE and NL ($74 \pm 9 \text{ m}^3\cdot\text{Mg}^{-1}$). The variability, as measured by the coefficient of variation, was higher for blue water (12%–126%) than for green water (7%–20%). The coefficient of variation for the combined green and blue WF of irrigated crops was 34% for potato, 25% for maize and 18% for sugar beet. The lowest coefficient of variation were for maize in CZ (9%) and potato in CY (10%); the highest were for maize in BE (19%) and sugar beet in IT (17%).

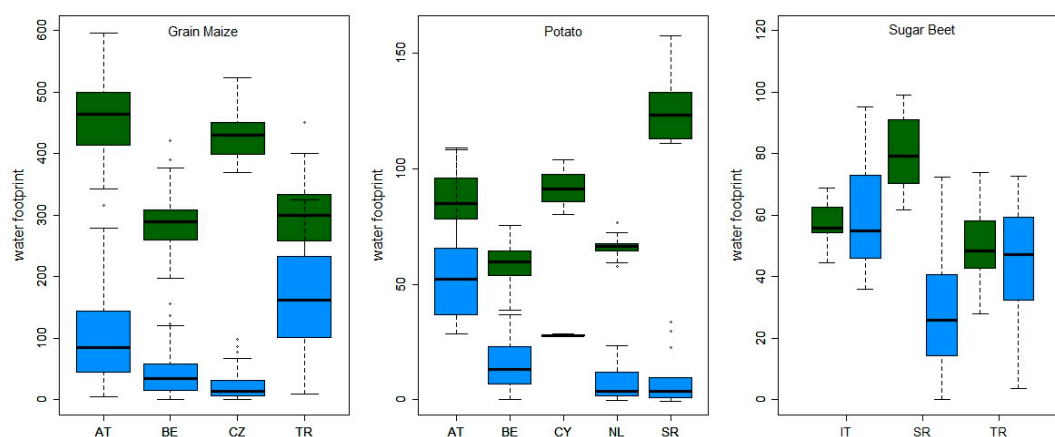


Figure 11. The blue water footprint (in $\text{m}^3\cdot\text{Mg}^{-1}$) for modelled yields of irrigated arable crops across the European regions for the period 1992–2012. A two letter code refers to the country that the region belongs to.

We calculated the grey water footprint on the basis of four different nitrogen application rates: a reported rate, a maximum rate derived from local field experiments, and a rate based on nutrient balance calculations according to Eurostat and World Bank (Figure 12). We assumed an equal occurrence of the four considered nitrogen application rates but with a maximum of 250 kg·N·ha⁻¹ in accordance with the European Nitrogen Directive. The highest potential nitrogen inputs are in NL and BE owing to a large share of animal manure in fertilizer application rates, followed by DE and NO with a much lower share of manure; the lowest nitrogen inputs are in TR and EE. For all regions the grey WF was larger for statistical yields than for modelled yields (Figure 13). An inter-annual and interregional comparison of the different crops showed the largest grey WF for oilseed rape (268 ± 100 m³·Mg⁻¹), barley (158 ± 72 m³·Mg⁻¹) and wheat (131 ± 39 m³·Mg⁻¹), followed by grain maize (91 ± 35 m³·Mg⁻¹) (Figure 13). The lowest grey WF was observed for sugar beet (13 ± 3 m³·Mg⁻¹) and potato (26 ± 7 m³·Mg⁻¹). The coefficient of variation (*cv*) for the grey WF calculated with statistical yields was 46% for barley, 38% for maize and rapeseed, 30% for wheat, 28% for potato and 22% for sugar beet; for the grey WF calculated with modelled yields the order was different: rapeseed (43%), barley (32%), wheat (30%), maize and potato (27%), and sugar beet (25%). Autumn sown crops showed large grey WFs, e.g., rapeseed in FI (409 ± 71 m³·Mg⁻¹), barley and wheat in CY (321 ± 131 m³·Mg⁻¹; 327 ± 209 m³·Mg⁻¹) and rapeseed in NL (310 ± 69 m³·Mg⁻¹). The lowest grey WFs were observed for sugar beet in all regions, ranging between 8 ± 1 m³·Mg⁻¹ in AT and 15 ± 2 m³·Mg⁻¹ in BE. The largest *cv* was for wheat in CY (64%) and maize in TR (57%), whereas the lowest *cv* occurred for potato in NL (9%) and sugar beet in DE (10%).

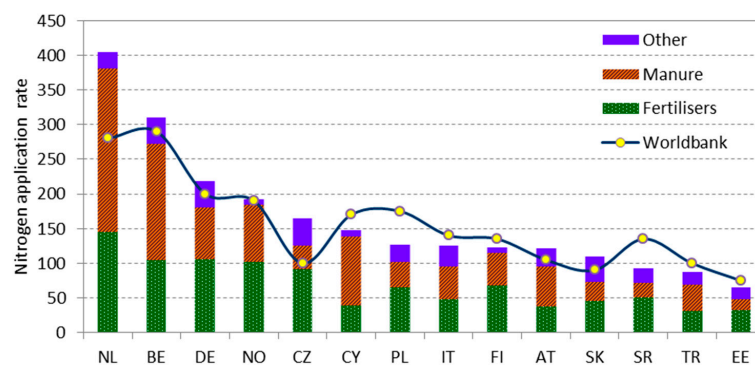


Figure 12. Nitrogen application rates on arable land (in kg·N·ha⁻¹) according to Eurostat [23] and World Bank [24] for the period 2006–2012. Other are soil amendments such as compost, sewage sludge and industrial waste. A two letter code refers to the country that the region belongs to.

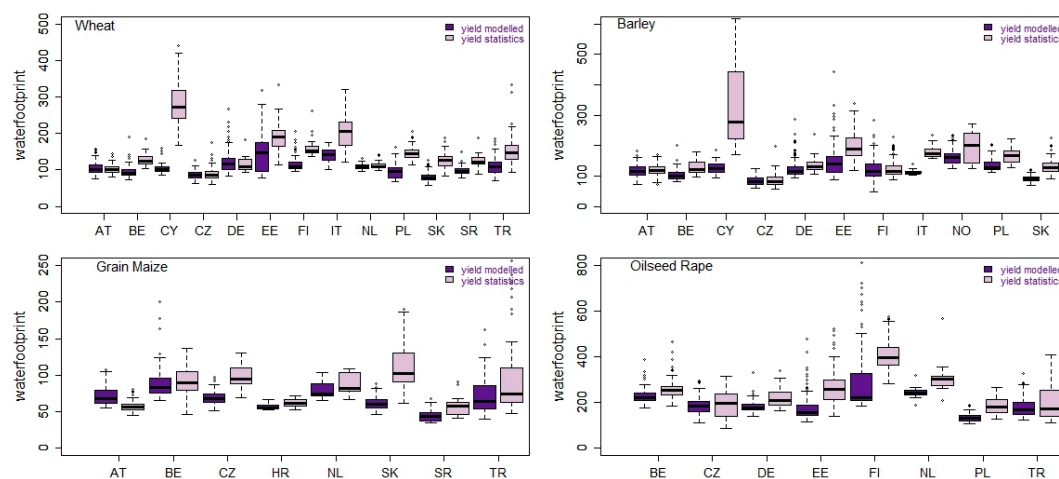


Figure 13. Cont.

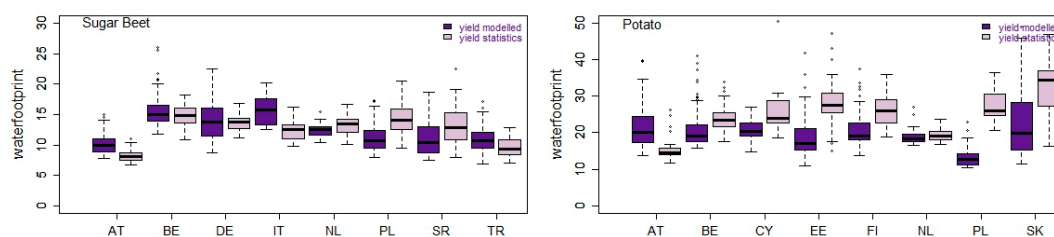


Figure 13. Grey water footprint (in $\text{m}^3 \cdot \text{Mg}^{-1}$) for modelled and statistical arable yields for the period 1992–2012 and for four different nitrogen application rates. Note the differences in scale between crops. A two letter code refers to the country that the region belongs to.

4. Discussion

We used the “Aquacrop” model to estimate crop growth and evapotranspiration under both rainfed and irrigated conditions. This model has been developed to simulate yield response to water under water-limited conditions [18–20]. Regions, crops and soils that are sensitive to dry spells and drought provide for a water-limited environment. Reviews of model behaviour show mixed results with respect to water use efficiencies and yields [28]. An intercomparison of eight models showed between 13% and 19% uncertainty in the estimation of evapotranspiration (“Aquacrop”: $cv = 15\%$), and between 13% and 34% for transpiration (“Aquacrop”: $cv = 24\%$) for wheat [21].

The green WF showed the largest variability for cereals ($cv = 51\%$ – 52%), closely followed by potato ($cv = 48\%$); the lowest variability was for oilseed rape ($cv = 36\%$) and sugar beet ($cv = 28\%$) (Table 3). For all arable crops, the yield is more variable ($\overline{cv} = 45\%$; cv in Table 2) than the crop evapotranspiration ($\overline{cv} = 21\%$; cv in Table 3). This clearly demonstrates the importance of yields and their variability for the water footprint. Similar to the findings of [29], root and tuber crops have much lower WFs as compared to cereals and oilseed crops (Table 3), owing to a combined effect of higher yields and higher moisture contents at harvest. Cereals and oilseed crops have a much smaller harvestable fraction of the total biomass produced per surface area, and therefore have larger water footprints.

Table 3. Green water footprint (WF) (WFg in $\text{m}^3 \cdot \text{Mg}^{-1}$) and evapotranspiration (ET in mm) for the major arable crops in Europe for the period 1992–2012. For crop abbreviations see Figure 3.

Crop	WFg·m	WFg·s	WFg·cv	ET·m	ET·s	ET·cv
RAP	1857	661	36	405	103	25
WHB	1108	580	52	459	87	19
WHD	1414	720	51	375	62	17
BAR	901	458	51	337	82	24
MAZ	590	304	52	373	73	20
POT	157	75	48	332	64	19
SBT	67	19	29	351	86	25

Notes: Where m denotes mean, s standard deviation and cv coefficient of variation (%).

Between the different regions in Europe, high yielding western European regions have WFs that can be up to six times lower than the WFs of regions in northern or southern Europe (Figures 9, 11 and 13). A threefold increase can occur between seasons, certainly in regions with variable yields. An analysis of variance (ANOVA) demonstrated clear effects of crops, countries, seasons and their factorial interactions on the green water footprint ($p < 0.001$). The largest variability between seasons is for the southern (CY, TR) and northern countries (EE, FI, NO) and for WHD, BAR and RAP. The variability between countries ($\overline{cv} = 14\%$; range: 7%–26%) is lower than the variability between seasons ($\overline{cv} = 22\%$; range: 10%–50%) and the variability between crops ($\overline{cv} = 46\%$; range: 29%–52%).

The breakdown of the crop water footprints in different components enabled a better understanding of the different contributing factors involved. A comparison between our calculations for the European regions and water footprint benchmarks for crop production provided by [16], revealed a good agreement for the green WF ($R^2 = 0.80$; $d = 0.95$), a reasonably good agreement for the blue WF ($R^2 = 0.64$; $d = 0.91$) and a lower agreement for the grey WF ($R^2 = 0.25$; $d = 0.73$), where R^2 is the coefficient of determination and d is the index of agreement [27]. Overall the best fit was obtained for the green WF (Figure 14). All WF were highly influenced by yield so that only well calibrated models able to model yield can be successfully deployed to estimate the WF. Yield variability determined the WF variability.

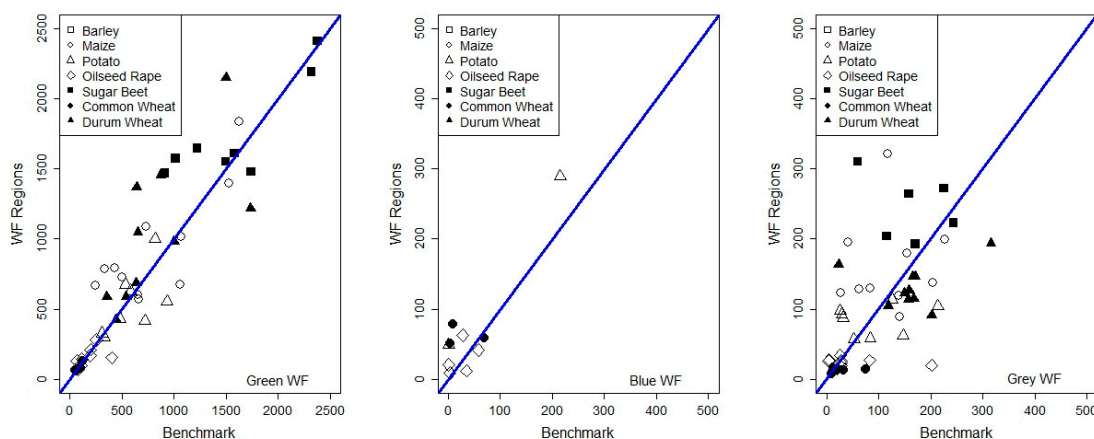


Figure 14. Comparison of green, blue and grey water footprints (WF) of this study with benchmark WF [16] in $\text{m}^3 \cdot \text{Mg}^{-1}$ for arable crops. The blue line represents the identity line.

Crop growth and production are mostly affected by the distribution of green water during the growing season. Blue water directly influences the yield provided water is available for irrigation: we modelled yield increases of up to 50% which highlight the benefits of irrigation. Water scarcity, exacerbated further by climate change, is an issue of major concern in arid and semi-arid regions with serious impacts on food security, sustainability and economy. The fact that the majority of available water is consumed by agricultural activities, particularly in arid and semi-arid countries, underpins the need for monitoring and reducing water consumption patterns in agricultural areas. Our modelled yield increases did not result in lower crop WFs under sprinkler irrigation; drip irrigation may result in lower WFs as calculated by [14]. The WF of agricultural crops allows for decision making and better management of the water potential.

Applied to agricultural production the grey WF is the amount of freshwater required for the assimilation of any pollutant, in casu nitrogen runoff due to agricultural crop production. Nitrogen application rates differ considerably between regions, and regulations are in place to limit the input for example in nitrogen vulnerable zones or nature conservation areas [30].

Other important sources of variation are crop type, farming system, soil type, and the rainfall-runoff regime. When runoff and drainage were taken into account (Figure 5), the grey WF showed a lot more variability between the years and could be as low as zero during some years for summer crops. In addition, the pollution and hence grey water is attributed to a single crop thereby neglecting the role of a crop in the rotation. For example oilseed rape had a high grey WF, despite the crop's capacity to deplete nitrogen from the previous crop before winter and therefore reduce N leaching. A contrary example is the high leaching risk of bare soil during winter prior to sugar beet. These effects were not incorporated in the applications of the grey water footprint of crops [13,16]. Recent applications concentrated on a nitrogen balance to budget uptake and losses, and arrived at higher estimates of nitrogen-related water pollution in river basins owing to differences

in computational methods [31]. Therefore the grey WF should be compared with caution between studies and agricultural systems.

Practices to reduce the WF of crop production start with awareness of the WF of different crop management systems. A transition to less water-demanding crops with higher water productivities or higher water use efficiencies offers opportunities to optimize plant water use. Soil and water conservation techniques and water saving irrigation methods, e.g., drip irrigation and deficit irrigation, could further reduce water demands [14]. Advanced techniques lower the crop water demand, but cannot markedly decrease the WF; achieving more stable and higher yields, however, can. The high dependency on yield warrants strategies to increase agricultural productivity which is accomplished through breeding programs and/or through optimizing resources use during the crop growth season. The grey WF is partly regularized through the Water Framework and Nitrates Directives with designated nitrate vulnerable zones and limitations on nitrogen and phosphorus applications [30]. Ensuring that water quality is minimally affected offers good perspectives for nutrient smart precision farming. Overall the water footprint and its assessment process helps establish a greater awareness of water consumption patterns among different stakeholders involved.

5. Conclusions

We calculated the green and blue water footprint with FAO's "Aquacrop" model, and the grey water footprint on the basis of nitrogen application rates for six major arable crops in 45 locations across Europe for the period 1992–2012. The WF of cereals is larger than the WF of tuber and root crops owing mainly to the difference in yield and moisture content at harvest between these crop types. Since yield has a larger variability than crop water use, yield estimates are of paramount importance to the crop WF. The WF for wheat, for example, can be up to five or six times larger in northern and southern Europe as compared to high yielding western European regions. The WF variability between crops was larger than the variability between seasons and in turn larger than the variability between countries. Yield increases under sprinkler irrigation were not high enough to reduce the water footprint. Water saving irrigation and soil conservation techniques, however, may result in WF reductions. The green and blue WF, but not the grey WF, compared favourably with internationally available benchmark values. Confronted with drainage and runoff, the grey WF tended to overestimate the contribution of nitrogen to the surface and groundwater. Other agro-hydrological methods to calculate the grey WF resulted in even larger values which points to caution when comparing different studies. The large variability between crops, regions and seasons; and between yields and water use as major components of the WF highlights the importance of crop yield variability. The water footprint is a measurable indicator that may support European water governance.

Acknowledgments: The authors acknowledge funding from COST ES1106, Belgian Science Policy contract number SD/RI/03A, JPI FACCE MACSUR (D.M. 24064/7303/15), 2812ERA 147 (from BLE Germany), the Czech project LD13030, the Ministry of Education, Youth and Sports of the Czech Republic within the National Sustainability Program I (NPU I), grant number LO1415, and contract nr III43007 of the Ministry of Education and Science of the Republic of Serbia. The authors thank their national meteorological services and institutes for providing weather data. Support for data collection is acknowledged from Sabina Thaler for Austrian data, Eva Pohanková for Czech data and Toprak Aslan for Turkish data.

Author Contributions: Anne Gobin, Kurt Christian Kersebaum, Josef Eitzinger and Mirek Trnka conceived and designed the experiments of calculating the water footprint. "Aquacrop" model runs were performed by Anne Gobin. All authors contributed to data collection and interpretation of the results.

Conflicts of Interest: The authors declare no conflict of interest.

Appendix A

The dominant soil type(s) and meteorological stations of each region are provided in Table A1, together with references to relevant datasets. Crop characteristics used for calibration are provided in Table A2.

Table A1. Soil hydrological properties of the topsoil for different locations across Europe.

CTRY	Location	Soil Type	Texture ¹	FC (%)	WP (%)	Pore Space	References
AT	Gross Enzersdorf	Chernozem	Silt Loam	35	21	43	[32]
AT	Gross Enzersdorf	Parachernozem	Sandy Loam	28	8	39	
AT	Gross Enzersdorf	Fluvisol	Clay Loam	35	22	42	
AT	Fuchsenbigl	Calcaric Chernozem	Silt Loam	38	23	53	
BE	Koksijde	Calcaric & Gleyic Fluvisol	Marine Clay	39	23	50	[33–35]
BE	Gent	Albeluvisol	Sandy Loam	22	10	47	
BE	Peer	Podzol	Loamy Sand	16	8	46	
BE	Ukkel	Luvisol	Silty Loam	34	12	49	
CY	Larnaca	Chromic Vertisol	Clay	42	28	50	[36,37]
CY	Nicosia	Vertic-Chromic Luvisol	Clay Loam	38	24	46	
CY	Pafos	Eutric Fluvisol	Loam	32	18	46	
CZ	Domaninek	Dystric Cambisol	Loam	30	15	47	[38]
CZ	Lednice	Chernozem	Silt Loam	35	16	49	
CZ	Verovany	Chernozem	Silt Loam	33	14	47	
DE	Manschnow	Fluvisol	Clay loam	39	15	46	[39]
DE	Manschnow	Cambisol	Sandy Loam	31	9	40	[39]
DE	Manschnow	Podzol	Sandy Loam	14	5	42	[39]
DE	Müncheberg	Eutric Cambisol	Loamy sand	26	11	36	[40,41]
DE	Braunschweig	Luvisol	Sandy Loam	24	6	46	[41]
EE	Kuusiku	Calcic Luvisol	Silt Loam	28	7	40	[42]
EE	Väike-Maarja	Calcaric Cambisol	Sandy Loam	28	8	45	
EE	Tartu	Mollic Cambisol	Loam	30	9	48	
EE	Võru	Stagnic Luvisol	Loamy Sand	20	6	42	
EE	Tallinn	Haplic Albeluvisol	Sand	16	3	44	
EE	Kuressaare	Gleysol	Clay	35	22	50	
EE	Pärnu	Gleysol	Clay loam	32	20	48	
FI	Jokioinen	Haplic Umbrisol	Silt loam	35	21	45	[43]
FI	Mikkeli	Mollic Cambisol	Sandy Loam	28	7	42	
FI	Ylistaro	Verti-Gleyic Cambisol	Silt Loam	35	15	48	
FI	Laukaa	Eutric Regosol	Silty Clay	46	25	55	
FI	Piikkiö	Vertic Cambisol	Clay Loam	36	22	48	
HR	Križevci	Gleyic Luvisol	Silt loam	36	12	41	[44]
IT	Foggia	Alluvial vertisol	Clay Loam	42	24	55	[45]
IT	Radicofani	Vertic Cambisol	Silty Clay	42	27	51	[46,47]
NL	Lelystad	Gleyic Fluvisol	Marine Clay	36	16	45	[48]
NO	Søråsjordet	Gleyic Podzoluvisol	Silt Loam	37	20	50	[49]
PL	Dąbrowice	Podzol	Loamy Sand	23	17	40	
SK	Jasl.Bohunice	Chernozem	Silty Loam	34	14	44	[50]
SK	Nitra	Luvisol	Clay Loam	36	17	44	
SK	Bratislava	Fluvisol	Sandy Loam	32	12	44	
SK	Hurbanovo	Phaeozem	Clay Loam	35	18	44	
SR	Rimski Sancevi	Chernozem	Loam	34	17	51	[51]
TR	Kirkklareli	Cambisol	Sandy Clay Loam	35	17	42	[52]
TR	Tekirdağ	Fluvisol	Sandy Clay Loam	39	28	46	[53]
TR	Edirne	Cambisol	Clay Loam	37	23	41	[53]

Notes: ¹ Soil texture is classified according to the USDA nomenclature.

Table A2. Planting (P) and harvesting (H) dates of arable crops in the different regions.

Region *	WHB/WHD	BAR	RAP	MAZ	POT	SBT
	P; H	P; H	P; H	P; H	P; H	P; H
AT	12/10; 30/7	25/3; 30/6		7/5; 26/9	16/4; 5/9	12/4; 18/8
BE	15/10; !/8	15/10; 15/7	15/9; 15/7	1/5; 30/9	10/4; 30/9	10/4; 15/10
CY	15/11; 30/5	15/11; 4/5			15/1; 24/5	
CZ	3/10; 30/7	30/3; 25/7	28/8; 20/7	30/4; 15/9		
DE-1	2/10; 30/7	20/9; 15/7	28/8; 24/7			16/5; 15/9
DE-2	25/10; 30/7	25/9; 25/6				15/4; 30/9
EE	30/8; 10/8	25/4; 3/8	1/5; 15/9		5/5; 10/9	
FI-1	30/8; 20/8	15/5; 20/8	15/5; 10/9		15/5; 10/9	
FI-2	10/9; 15/8	10/5; 15/8	10/5; 1/9		15/5; 5/9	
HR				29/4; 3/10		
IT-1	15/11; 20/6					22/3; 18/8
IT-2	15/11; 15/7	15/11; 10/7				

Table A2. Cont.

Region *	WHB/WHD	BAR	RAP	MAZ	POT	SBT
	P; H	P; H	P; H	P; H	P; H	P; H
NL	20/10; 30/7		5/9; 17/7	30/4; 15/10	25/4; 20/9	10/4; 15/10
NO		25/4; 15/8				
PL	20/9; 14/7	24/4; 16/7	28/8; 17/8		15/4; 30/9	15/4; 20/9
SK	7/10; 20/7	24/3; 10/7		20/4; 3/9	15/4; 15/9	
SR	15/11; 10/7			20/4; 30/9	30/3; 10/7	30/3; 15/10
TR	15/11; 30/6		30/9; 15/6	9/4; 20/8		15/3; 20/8

Notes: * For the name of the region see Table A1.

References

1. Hoekstra, A.Y.; Mekonnen, M.M. The water footprint of humanity. *Proc. Natl. Acad. Sci. USA* **2012**, *109*, 3232–3237. [[CrossRef](#)] [[PubMed](#)]
2. Ciais, P.; Reichstein, M.; Viovy, N.; Granier, A.; Ogée, J.; Allard, V.; Aubinet, M.; Buchmann, N.; Bernhofer, C.; Carrara, A.; et al. Europe-wide reduction in primary productivity caused by the heat and drought in 2003. *Nature* **2005**, *437*, 529–533. [[CrossRef](#)] [[PubMed](#)]
3. COPA-COGECA. COPA-COGECA. Assessment of the impact of the heat wave and drought of the summer of 2003 on agriculture and forestry. In *Fact Sheets of the Committee of Agricultural Organisations in the European Union and the General Committee for Agricultural Cooperation in the European Union*; COPA-COGECA: Brussels, Belgium, 2003.
4. Dai, A. Increasing drought under global warming in observations and models. *Nat. Clim. Chang.* **2013**, *3*, 52–58. [[CrossRef](#)]
5. Trnka, M.; Olesen, J.E.; Kersebaum, K.C.; Skjelvag, A.O.; Eitzinger, J.; Seguin, B.; Peltonen Sainio, P.; Rotter, R.; Iglesias, A.; Orlandini, S.; et al. Agroclimatic conditions in Europe under climate change. *Glob. Chang. Biol.* **2011**, *17*, 2298–2318. [[CrossRef](#)]
6. Trnka, M.; Hlavinka, P.; Semenov, M.A. Adaptation options for wheat in Europe will be limited by increased adverse weather events under climate change. *J. R. Soc. Interface* **2015**, *12*, 20150721. [[CrossRef](#)] [[PubMed](#)]
7. Damerau, K.; Patt, A.G.; van Vliet, O.P. Water saving potentials and possible trade-offs for future food and energy supply. *Glob. Environ. Chang.* **2016**, *39*, 15–25. [[CrossRef](#)]
8. Allan, J.A. Virtual water: A strategic resource, global solutions to regional deficits. *Ground Water* **1998**, *36*, 545–546. [[CrossRef](#)]
9. Zoumides, C.; Bruggeman, A.; Hadjidakou, M.; Zachariadis, T. Policy-relevant indicators for semi-arid nations: The water footprint of crop production and supply utilization of Cyprus. *Ecol. Indic.* **2014**, *43*, 205–214. [[CrossRef](#)]
10. Ridoutt, B.G.; Pfister, S. A revised approach to water footprinting to make transparent the impacts of consumption and production on global freshwater scarcity. *Glob. Environ. Chang.* **2010**, *20*, 113–120. [[CrossRef](#)]
11. International Organization for Standardization. *ISO 14046: 2014: Environmental Management: Water Footprint—Principles, Requirements and Guidelines*; International Organization for Standardization: Geneva, Switzerland, 2014.
12. Chenoweth, J.; Hadjidakou, M.; Zoumides, C. Quantifying the human impact on water resources: A critical review of the water footprint concept. *Hydrol. Earth Syst. Sci.* **2014**, *18*, 2325–2342. [[CrossRef](#)]
13. Mekonnen, M.M.; Hoekstra, A.Y. The green, blue and grey water footprint of crops and derived crop products. *Hydrol. Earth Syst. Sci.* **2011**, *15*, 1577–1600. [[CrossRef](#)]
14. Chukalla, A.D.; Krol, M.S.; Hoekstra, A.Y. Green and blue water footprint reduction in irrigated agriculture: Effect of irrigation techniques, irrigation strategies and mulching. *Hydrol. Earth Syst. Sci.* **2015**, *19*, 4877–4891. [[CrossRef](#)]
15. Zhuo, L.; Mekonnen, M.M.; Hoekstra, A.Y. The effect of inter-annual variability of consumption, production, trade and climate on crop-related green and blue water footprints and inter-regional virtual water trade: A study for China (1978–2008). *Water Res.* **2016**, *94*, 73–85. [[CrossRef](#)] [[PubMed](#)]

16. Mekonnen, M.M.; Hoekstra, A.Y. Water footprint benchmarks for crop production: A first global assessment. *Ecol. Indic.* **2014**, *46*, 214–223. [[CrossRef](#)]
17. Allen, R.G.; Pereira, L.S.; Raes, D.; Smith, M. *Crop Evapotranspiration—Guidelines for Computing Crop Water Requirements*; FAO Irrigation and Drainage Paper; Food and Agriculture Organization: Rome, Italy, 1998; p. D05109.
18. FAO Crop-Model to Simulate Yield Response to Water. Available online: <http://www.fao.org/nr/water/aquacrop.html> (accessed on 23 August 2016).
19. Steduto, P.; Hsiao, T.C.; Raes, D.; Fereres, E. AquaCrop—The FAO crop model to simulate yield response to water: I. Concepts and underlying principles. *Agron. J.* **2009**, *101*, 426–437. [[CrossRef](#)]
20. Raes, D.; Steduto, P.; Hsiao, T.C.; Fereres, E. Aquacrop the FAO crop model to simulate yield response to water: II. Main algorithms and software description. *Agron. J.* **2009**, *101*, 438–447. [[CrossRef](#)]
21. Kersebaum, K.C.; Kroes, J.; Gobin, A.; Takác, J.; Hlavinka, P.; Trnka, M.; Ventrella, D.; Giglio, L.; Ferrise, R.; Moriondo, M.; et al. Assessing the uncertainty of model based water footprint estimation using an ensemble of crop growth models on winter wheat. *Water* **2016**, *8*, 571. [[CrossRef](#)]
22. Rockström, J.; Falkenmark, M.; Karlberg, L.; Hoff, H.; Rost, S.; Gerten, D. Future water availability for global food production: The potential of green water for increasing resilience to global change. *Water Res.* **2009**, *45*, W00A12. [[CrossRef](#)]
23. Eurostat. Gross Nutrient Balance. Available online: http://ec.europa.eu/eurostat/cache/metadata/EN/aei_pr_gnb_esms.htm (accessed on 23 August 2016).
24. World Bank, Fertilizer Consumption Rates per Hectare of Arable Land. Available online: <http://databank.worldbank.org/data/reports.aspx?source=2&series=AG.CON.FERT.ZS&country> (accessed on 23 August 2016).
25. Eurostat. Handbook for Annual Crop Statistics. European Commission-Eurostat, Directorate E Sectoral and Regional Statistics, Unit E1 Agriculture and Fisheries. Available online: http://ec.europa.eu/eurostat/cache/metadata/Annexes/apro_acs_esms_an1.pdf (accessed on 23 August 2016).
26. R Core Group. The R Project for Statistical Computing. Available online: <https://www.r-project.org/> (accessed on 20 November 2016).
27. Zambrano-Bigiarini, M. hydroGOF: Goodness-of-Fit Functions for Comparison of Simulated and Observed Hydrological Time Series. 2011. R Package Version 0.3-2. Available online: <http://CRAN.R-project.org/package=hydroGOF> (accessed on 23 August 2016).
28. Evett, S.R.; Tolk, J.A. Introduction: Can Water Use Efficiency Be Modeled Well Enough to Impact Crop Management? *Agron. J.* **2009**, *101*, 423–425. [[CrossRef](#)]
29. Mekonnen, M.M.; Hoekstra, A.Y. The Green, Blue and Grey Water Footprint of Crops and Derived Crop Products. Value of Water Research Report Series No. 47; UNESCO-IHE: Delft, The Netherlands, 2010. Available online: <http://www.waterfootprint.org/Reports/Report47-WaterFootprintCrops-Vol1.pdf> (accessed on 23 August 2016).
30. Velthof, G.L.; Lesschen, J.P.; Webb, J.; Pietrzak, S.; Miatkowski, Z.; Pinto, M.; Kros, J.; Oenema, O. The impact of the Nitrates Directive on nitrogen emissions from agriculture in the EU-27 during 2000–2008. *Sci. Total Environ.* **2014**, *468*, 1225–1233. [[CrossRef](#)] [[PubMed](#)]
31. Mekonnen, M.M.; Hoekstra, A.Y. Global gray water footprint and water pollution levels related to anthropogenic nitrogen loads to fresh water. *Environ. Sci. Technol.* **2015**, *49*, 12860–12868. [[CrossRef](#)] [[PubMed](#)]
32. Eitzinger, J.; Trnka, M.; Semerádová, D.; Thaler, S.; Svobodová, E.; Hlavinka, P.; Siska, B.; Takáč, J.; Malatinská, L.; Nováková, M.; et al. Regional climate change impacts on agricultural crop production in Central and Eastern Europe—hotspots, regional differences and common trends. *J. Agric. Sci.* **2013**, *151*, 787–812. [[CrossRef](#)]
33. Gobin, A. Impact of heat and drought stress on arable crop production in Belgium. *Natl. Hazards Earth Syst. Sci.* **2012**, *12*, 1911–1922. [[CrossRef](#)]
34. Gobin, A. Modelling climate impacts on arable yields in Belgium. *Clim. Res.* **2010**, *44*, 55–68. [[CrossRef](#)]
35. Gobin, A. The water footprint of Belgian arable crops. *Ital. J. Agric. Meteorol.* **2015**, *4*, 91–97.
36. Zoumides, C.; Bruggeman, A.; Zachariadis, T.; Pashiardis, S. Quantifying the poorly known role of groundwater in agriculture: The case of Cyprus. *Water Resour. Manag.* **2013**, *27*, 2501–2514. [[CrossRef](#)]

37. Camera, C.; Zomeni, Z.; Noller, J.; Zissimos, A.; Christoforou, I.; Bruggeman, A. A high resolution map of soil types and physical properties for Cyprus: A digital soil mapping optimization. *Geoderma* **2017**, *285*, 35–49. [[CrossRef](#)]
38. Hlavinka, P.; Trnka, M.; Kersebaum, K.; Cermak, P.; Pohankova, E.; Ors_ag, M.; Pokorný, E.; Fischer, M.; Brtnický, M.; Zalud, Z. Modelling of yields and soil nitrogen dynamics for crop rotations by HERMES under different climate and soil conditions in the Czech Republic. *J. Agric. Sci.* **2014**, *152*, 188–204. [[CrossRef](#)]
39. Kersebaum, K.C.; Nendel, C. Site-specific impacts of climate change on wheat production across regions of Germany using different CO₂ response functions. *Eur. J. Agron.* **2014**, *52*, 22–32. [[CrossRef](#)]
40. Mirschel, W.; Barkusky, D.; Hufnagel, J.; Kersebaum, K.C.; Nendel, C.; Laacke, L.; Luzi, K.; Rosner, G. Coherent multi-variable field data set of an intensive cropping system for agro-ecosystem modelling from Müncheberg, Germany. *Open Data J. Agric. Res.* **2016**, *2*, 1–10. [[CrossRef](#)]
41. Kollas, C.; Kersebaum, K.C.; Nendel, C.; Manevski, K.; Müller, C.; Palosuo, T.; Armas-Herrera, C.M.; Beaudoin, N.; Bindi, M.; Charfeddine, M.; et al. Crop rotation modelling—a European model intercomparison. *Eur. J. Agron.* **2015**, *70*, 98–111. [[CrossRef](#)]
42. Kadaja, J.; Saue, T. Effects of different irrigation and drainage regimes on yield and water productivity of two potato varieties under Estonian temperate climate. *Agric. Water Manag.* **2016**, *165*, 61–71. [[CrossRef](#)]
43. Peltonen-Sainio, P.; Jauhiainen, L.; Hakala, K. Crop responses to temperature and precipitation according to long-term multi-location trials at high-latitude conditions. *J. Agric. Sci.* **2011**, *149*, 49–62. [[CrossRef](#)]
44. Vučetić, V. Modelling of maize production in Croatia: Present and future climate. *J. Agric. Sci.* **2011**, *149*, 145–157. [[CrossRef](#)] [[PubMed](#)]
45. Ventrella, D.; Stellacci, A.M.; Castrignanò, A.; Charfeddine, M.; Castellini, M. Effects of crop residue management on winter durum wheat productivity in a long term experiment in Southern Italy. *Eur. J. Agron.* **2016**, *77*, 188–198. [[CrossRef](#)]
46. Dalla Marta, A.; Orlando, F.; Mancini, M.; Guasconi, F.; Motha, R.; Qu, J.; Orlandini, S. A simplified index for an early estimation of durum wheat yield in Tuscany (Central Italy). *Field Crops Res.* **2015**, *170*, 1–6. [[CrossRef](#)]
47. Guasconi, F.; Dalla Marta, A.; Grifono, D.; Mancini, M.; Orlando, F.; Orlandini, S. Influence of climate on durum wheat production and use of remote sensing and weather data to predict quality and quantity of harvests. *Ital. J. Agrometeorol.* **2011**, *3*, 21–28.
48. Van Bakel, P.J.T.; Massop, H.T.L.; Kroes, J.G.; Hoogewoud, J.; Pastoors, R.; Kroon, T. Actualisatie Hydrologie voor STONE 2.3. In *Aanpassing Randvoorwaarden en Parameters, Koppeling Tussen NAGROM en SWAP, en Plausibiliteitstoets*; WOt-Rapport 57; Wettelijke Onderzoekstaken Natuur & Milieu (MNP), Alterra: Wageningen, The Netherlands, 2008.
49. Deelstra, J.; Kværnø, S.H.; Skjevdal, R.; Vandsemb, S.; Eggestad, H.O.; Ludvigsen, G.H. *A General Description of Skuterud Catchment*; Jordforsk (Now NIBIO) Report No. 61/05; Bioforsk: Ås, Norway, 2005.
50. Takáč, J.; Skalský, R.; Morávek, A.; Klikušovská, Z.; Bezák, P.; Bárđyová, M. Spatial Patterns of Agricultural Drought Events in Danube Lowland in the 1961–2013 Period. In *Proceedings of the International Scientific Conference towards Climatic Services*, Nitra, Slovakia, 15–18 September 2015.
51. Stričević, R.; Cosić, M.; Djurović, N.; Pejić, B.; Maksimović, L. Assessment of the FAO “Aquacrop” model in the simulation of rainfed and supplementally-irrigated maize, sugar beet and sunflower. *Agric. Water Manag.* **2011**, *98*, 1615–1621.
52. Şaylan, L.; Çaldağ, B.; Bakanoğulları, F. *Investigation of Potential Effects of Climate Change on Crop Growth by Crop Growth Simulation Models*; TUBITAK Project No.: 1080567; TUBITAK: Istanbul, Turkey, 2012; p. 258. (In Turkish)
53. Çakir, R. Istranca (Yıldız) Dağı Güneyinde Yer Alan Vertisol Ordosu Topraklarının Toprak Taksonomisine Göre Belirlenmesi, Toprak ve Su Mühendisliği Yönünden İrdelenmesi. Ph.D. Thesis, Trakya Üniversitesi, Edirne, Turkey, 1997.

